

# Phase diagram of the quarter-filled extended Hubbard model on a two-leg ladder

Matthias Vojta<sup>(a)\*</sup>, Arnd Hübsch<sup>(b)</sup>, and R. M. Noack<sup>(c)</sup>

(a) Department of Physics, Yale University, New Haven, CT 06520-8120, USA

(b) Institut für Theoretische Physik, Technische Universität Dresden, D-01062 Dresden, Germany

(c) Institut für Physik, Johannes-Gutenberg-Universität Mainz, D-55099 Mainz, Germany

(December 2, 2024)

We investigate the ground-state phase diagram of the quarter-filled two-leg Hubbard ladder with additional nearest-neighbor Coulomb repulsion  $V > 0$  using the Density Matrix Renormalization Group technique. We find that the system is insulating at any finite  $V$ . The ground-state is homogeneous at small  $V$ , a “checkerboard” charge-ordered insulator at large  $V$  and not too small  $U$ , and is phase-separated for moderate or large  $V$  and small  $U$ . The zero temperature transition between the homogeneous and the charge-ordered phase is found to be second order. In both phases the existence of a spin gap mainly depends on the ratio of interchain to intrachain hopping. In the limit of strong coupling, we construct an effective Hamiltonian for the spin degrees of freedom in the charge-ordered phase which maps the system onto a frustrated spin chain. The opening of a spin gap is thus connected with spontaneous dimerization.

## I. INTRODUCTION

Quasi-one-dimensional systems present a unique opportunity to study the interplay between strong quantum fluctuations on the one hand and a tendency to charge or spin ordering on the other. Examples include Peierls or spin-Peierls behavior as well as charge ordering due to electron-electron interaction. One material in which such behavior has been found is the two-leg ladder material  $\text{NaV}_2\text{O}_5$ .  $\text{NaV}_2\text{O}_5$  undergoes a phase transition at  $T_c = 34$  K that is characterized by the opening of a spin gap and a doubling of the unit cell. Although this transition was originally thought to be spin-Peierls, recent studies have found evidence for charge order.<sup>1-3</sup> Above the transition, the material seems to be best described as a quarter-filled ladder.<sup>4,5</sup> Such two-leg-ladder structures have also been found in a number of other materials, including the Vanadates  $\text{MgV}_2\text{O}_5$  and  $\text{CaV}_2\text{O}_5$ , and the cuprates  $\text{SrCu}_2\text{O}_3$  and  $\text{Sr}_{14}\text{Cu}_{24}\text{O}_{41}$ . For a more detailed description of ladder materials and models as well as a discussion of the extensive theoretical work on ladder models, we direct the reader to a recent review<sup>6</sup> and the references contained therein.

In  $\text{NaV}_2\text{O}_5$ , the character of the charge ordering and the nature of the transition are currently under debate. While evidence is growing<sup>7-9</sup> that the charge-ordered state has a zigzag-like charge arrangement, the question of whether this charge ordering is continuous or discontinuous has not yet been settled experimentally. Theoretically, the magnetic properties of the compound for  $T < T_c$  have been calculated for different charge-ordering patterns<sup>10,11</sup> and compared to experiments. Again, zigzag charge ordering on ladders (possibly with intervening disordered ladders<sup>12</sup>) leads to magnon dispersions in good agreement with neutron scattering data. Additionally, the possibility of two separate transitions at nearby temperatures has been raised,<sup>13,14</sup> in this sce-

nario the charge order would set in at one temperature while the spin gap would open at a second, lower critical  $T$ . Very recently, a scenario of singlet cluster formation instead of zigzag charge ordering has been suggested.<sup>15</sup> However, this model seems not to be able to reproduce the experimentally found spin gap and magnon dispersion data.<sup>16</sup> It is clear that more experimental work is necessary to clarify the nature of the low-temperature phase of  $\text{NaV}_2\text{O}_5$ .

One of the simplest models of interacting electrons that allows for charge ordering is the extended Hubbard model, i.e. the Hubbard model supplemented by an additional nearest-neighbor (NN) Coulomb repulsion,  $V$ . This model has been studied in one dimension (1D) in the strong-coupling limit,<sup>17</sup> at quarter filling<sup>18,19</sup> and at half filling<sup>20-23</sup> and in between,<sup>24,25</sup> in the 2D system at half filling,<sup>26,27</sup> and within the Dynamical Mean Field Theory (the limit of infinite dimensions) at quarter<sup>28</sup> and half filling.<sup>29</sup> A variety of techniques, such as mean-field approximations, perturbation theory, as well as numerical methods as quantum Monte Carlo and the Density Matrix Renormalization Group (DMRG) have been employed.

The result of investigations of the charge-order transition can be summarized as follows: At the mean-field level, the transition between a homogeneous state and a charge-density wave (CDW) state at half filling in a hypercubic lattice occurs at  $V_c = U/z_0$ , where  $z_0$  denotes the number of nearest neighbors ( $z_0 = 2d$ ). Numerical studies<sup>21,22</sup> indicate a slightly higher value of  $V_c$ , at least in 1D. Interestingly, the transition at half filling in 1D has been found to be second order at small  $U/t$  and first order at large  $U/t$  with the tricritical point located at  $U_c/t \sim 4 - 6$ .<sup>22,23</sup> Here we use the term “first order” to denote discontinuous behavior of the charge order parameter as a function of microscopic parameters such as  $V$  or band filling, and “second order” to denote continuous be-

havior. For fillings below half-filling in 1D, the situation is more complicated because a number of phases compete at large  $V$ .<sup>18,19,25</sup> For dimension larger than one, indications are that the charge-order transition is generally first order.<sup>26–29</sup> However, conclusive studies that can reliably distinguish between first- and second-order transitions are lacking. At small  $U$  and large  $V$ , the extended Hubbard model undergoes phase separation (PS) rather than a transition to a CDW state. For the 1D model between quarter- and half-filling, it has been established<sup>25</sup> that PS occurs for  $|U|/t < 4$  in the  $V = \infty$  limit, whereas for  $U/t > 4$  the system undergoes a transition to a  $q = \pi$  CDW state for sufficiently large  $V$ .<sup>24</sup> Phase separation in higher dimensions has also been discussed.<sup>30</sup>

For the 1D system in particular there has been recent interest in the possibility of dominant superconducting correlations in the uniform ground-state away from half-filling when  $V \gg U \sim t$ ,<sup>19,25</sup> i.e., in the proximity of the phase-separated region. We note here that the uniform phase in 1D off half-filling is metallic and can in general be described within the Luttinger liquid picture. Although dominant superconducting correlations have not been established in the ground state of the 1D extended Hubbard model to date, a number of non-Luttinger-liquid effects have been observed<sup>25</sup>.

Some of the present authors have previously studied<sup>31</sup> the charge-order transition in the extended Hubbard model on the two-leg ladder at various band fillings for  $U/t = 4$  and  $8$ . A transition to a checkerboard charge-ordered state was found for all fillings between quarter- and half-filling. The transition is second-order near quarter filling and first-order near half-filling for sufficiently large  $U$ .

The focus of the present paper is on this model at quarter filling. We study the phase diagram as a function of  $U/t$  and  $V/t$  for repulsive  $U$  and  $V$  and discuss the properties of the ground state phases as well as the nature of the phase transitions. One of our main results, the phase diagram for the case of isotropic hopping deduced from the numerical calculations, is shown in Fig. 1. At large  $U$  and  $V$  we find an insulating checkerboard charge-ordered state as expected. Interestingly, the charge-ordered state can have gapless or gapped spin excitations depending on the ratio of  $V/U$ . The precise location of the boundary at which the spin gap closes in the intermediate coupling regime could not be obtained by the methods used here. We have indicated this uncertainty by a question mark in the phase diagram. At small  $U$  and large  $V$  the system shows phase separation, whereas it is insulating with a vanishing spin gap in the weak-coupling region at small  $U > 0$ ,  $V > 0$  (which extends to large  $U$  at small  $V$ ). Schematic phase diagrams for different values of the hopping anisotropy can be found in Fig. 14 of Sec. IV.

The paper is organized as follows: In Sec. II, we introduce the extended Hubbard model and discuss some results known for the  $V = 0$  case, i.e., the “bare” Hubbard model on a two-leg ladder. In Sec. III, we present numerical results for the extended Hubbard model. We

discuss the properties of the phases shown in Fig. 1, and examine the transition to the charge-ordered state. At large  $V$ , where charge order is well established, it is possible to derive an effective Hamiltonian for the residual spin degrees of freedom; this is done in Sec. IV. A summary and a discussion of the relevance of our results to experimental systems (especially  $\text{NaV}_2\text{O}_5$ ) terminates the paper.

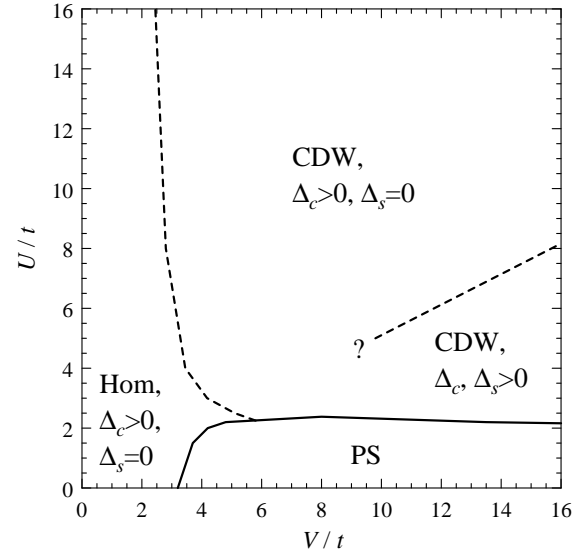


FIG. 1. Ground state phase diagram of the extended quarter-filled Hubbard model on a two-leg ladder with isotropic hopping. The axes denote the strength of the on-site and nearest-neighbor repulsion,  $U/t$  and  $V/t$ . The dashed lines represent second order phase transitions. The solid line marks the boundary of the phase separation region (PS) where the thermodynamic compressibility diverges. The quantities  $\Delta_c$  and  $\Delta_s$  are gaps for charge and spin excitations, defined in Eq. (5).

## II. EXTENDED HUBBARD MODEL

The single-band extended Hubbard model has the Hamiltonian

$$H = - \sum_{\langle ij \rangle \sigma} t_{ij} (c_{i\sigma}^\dagger c_{j\sigma} + h.c.) + U \sum_i n_{i\uparrow} n_{i\downarrow} + \sum_{\langle ij \rangle} V_{ij} n_i n_j . \quad (1)$$

Here we consider a lattice consisting of two chains of length  $L$ , i.e., a ladder, and restrict ourselves to the band filling  $\langle n \rangle = N/(2L) = 1/2$ , where  $N$  is the number of electrons. The summation  $\langle ij \rangle$  runs over all pairs of nearest-neighbor sites on the ladder, taking open boundary conditions between the chains. The hopping matrix elements along the legs and rungs of the ladder are denoted  $t_{\parallel}$  and  $t_{\perp}$ , respectively, and the nearest-neighbor Coulomb interactions are similarly denoted  $V_{\parallel}$  and  $V_{\perp}$ .

Unless otherwise noted, we will use  $t_{\parallel}$  as unit of energy. In this work, we will treat primarily the “isotropic” case,  $t_{\parallel} = t_{\perp} = t$  and  $V_{\parallel} = V_{\perp} = V$ .

The non-interacting Hamiltonian ( $U = V = 0$ ) can be diagonalized by a Fourier transform (for periodic boundary conditions in the chain direction), leading to the single-particle energies

$$\epsilon_{\mathbf{q}} = -2t_{\parallel} \cos q_x + t_{\perp} \cos q_y \quad (2)$$

where  $\mathbf{q} = (q_x, q_y)$ ,  $q_x$  is the momentum along the chains and the momenta  $q_y = 0, \pi$  correspond to bonding and antibonding symmetry, respectively. Either one or both of the bands can be occupied in the noninteracting system, depending on the total particle density and the ratio of  $t_{\perp}$  and  $t_{\parallel}$ . At quarter filling, the transition occurs at isotropic hopping: for  $t_{\perp} < t_{\parallel}$  both bands are less than half-filled, whereas for  $t_{\perp} > t_{\parallel}$  the bonding band is half-filled and the antibonding band is unoccupied.

The effect of the Hubbard interaction  $U$  on this system has been extensively studied. In the weak-coupling limit,  $U \ll t$ , the phase diagram has been investigated using the perturbative renormalization group (RG).<sup>32</sup> A variety of phases have been shown to exist as a function of band filling and hopping anisotropy. In general, the two-band system can have four possible modes (symmetric and antisymmetric charge and spin modes), each of which can be either massive or massless. The phases can therefore be classified using the notation  $CnSm$  where  $n$  and  $m$  designate the number of gapless charge and spin modes, respectively ( $0 \leq n, m \leq 2$ ). At quarter filling, the weak-coupling RG<sup>32</sup> for the “bare” Hubbard model ( $V = 0$ ) yields the following results: For  $t_{\perp} > t_{\parallel}$  the system behaves as a half-filled Luttinger liquid; Umklapp scattering in the bonding channel is a relevant perturbation which leads to a charge-gapped C0S1 phase at small  $U$ . In contrast, deep in the two-band region,  $t_{\perp} \ll t_{\parallel}$ , one finds a metallic C1S0 phase in the weak-coupling limit. Near isotropic hopping, the bottom of the antibonding band just “touches” the Fermi surface, and the curvature of the dispersion becomes important, leading to additional narrow regions of C2S2 and C2S1 phases. Several of these weak-coupling predictions have been verified by numerical DMRG calculations in the intermediate and strong coupling regimes for a wide range of filling.<sup>33</sup> Systematic studies of the phases of the *extended* Hubbard model on a two-leg ladder away from half-filling have to our knowledge not yet been carried out.

The numerical results in this paper have been calculated with the DMRG technique<sup>34</sup> on lattices of up to  $2 \times 80$  sites with open boundary conditions at the ends of the chains as well as between the two chains. Most data shown are obtained by keeping 600 states per block, resulting in the sum of the discarded density matrix eigenvalues being typically  $10^{-8}$  or less. For small system sizes we have checked the convergence by using up to 1000 states per block. Unless otherwise noted, we estimate

the errors in the gap energies and correlation functions obtained using the DMRG procedure to be less than a few percent.

### III. NUMERICAL RESULTS

In this section we present the results of our numerical investigations and discuss the characteristics of the phases shown in Fig. 1. Important ground-state properties are the static charge and spin correlation functions. Using the DMRG technique we have calculated the static charge structure factor

$$C(\mathbf{q}) = \frac{1}{2L} \sum_i e^{i\mathbf{q} \cdot \mathbf{R}_i} \bar{C}(\mathbf{R}_i) \quad (3)$$

where

$$\bar{C}(\mathbf{R}_i) = \frac{1}{N_{\text{av}}} \sum_{\{j\}} \langle \delta n_{j+i} \delta n_j \rangle, \quad (4)$$

$\langle \dots \rangle$  denotes the ground-state expectation value,  $\delta n_j = n_j - \langle n_j \rangle$ , and we average over typically  $N_{\text{av}} = 6$  sites to remove oscillations due to the open boundaries. For checkerboard charge order, which is expected to be the ground state for large values of  $V$ ,  $C(\mathbf{q})$  should show a pronounced peak at  $\mathbf{Q} = (\pi, \pi)$ . The spin order can be studied by looking at the spin structure factor,  $S(\mathbf{q})$ , which is defined similarly in terms of the spin–spin correlation function  $\langle S_{j+i}^z S_j^z \rangle$ .

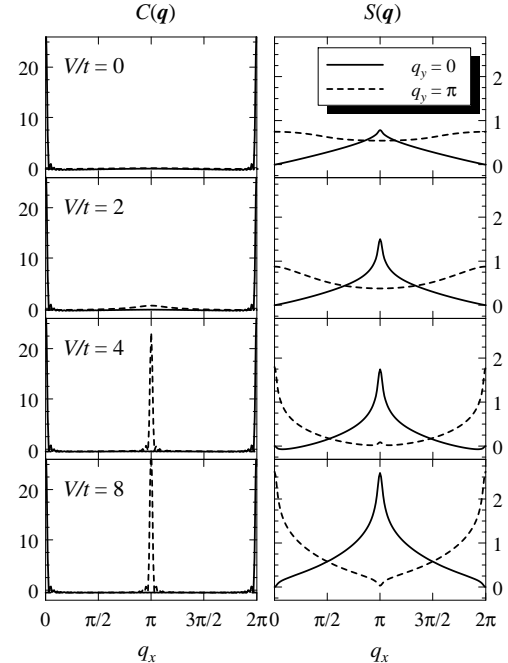


FIG. 2. Charge and spin correlation functions for a  $64 \times 2$  ladder, isotropic hopping  $t_{\parallel} = t_{\perp} = t$ ,  $U/t = 8$ , quarter filling  $\langle n \rangle = 0.5$  (64 electrons), and various values of the nearest-neighbor repulsion  $V$ .

In Fig. 2, we exhibit  $C(\mathbf{q})$  and  $S(\mathbf{q})$  for a  $2 \times 64$  system at  $U/t = 8$  at quarter filling for different values of  $V$ . The transition between a homogeneous state at small  $V$  and an ordered CDW state at large  $V$  can clearly be seen. The DMRG ground state at  $V > V_c$  has broken translation invariance, i.e., for large  $V$  every second site is empty. (Here,  $V_c/t = 2.8 \pm 0.1$ .) In the spin channel, peaks at  $(0, \pi)$  and  $(\pi, 0)$  develop with increasing  $V$  showing an alternating spin pattern on the *occupied* sites in the CDW state. This spin order arises from virtual hopping processes (fourth order in  $t$ ) which lead to antiferromagnetic couplings between the occupied sites. In the limit of large  $V$ , the system can be mapped to a  $J_1-J_2$  spin- $\frac{1}{2}$  chain; this will be discussed in Sec. IV.

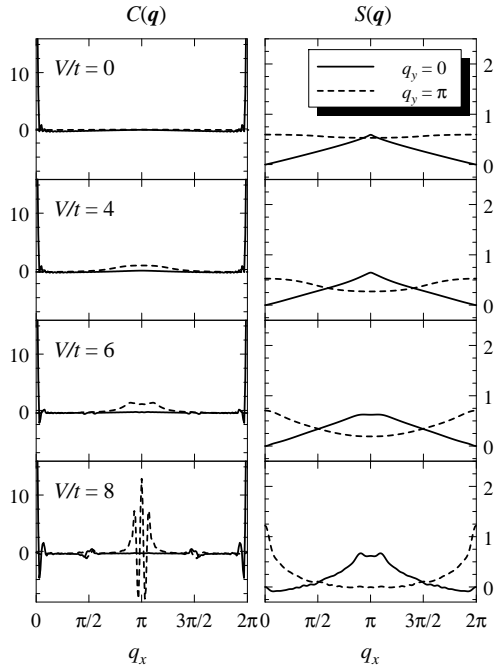


FIG. 3. As Fig. 2, but for  $U = 2t$ . The rapid oscillations in  $C(\mathbf{q})$  at  $V/t = 8$  indicate that increasing  $V$  drives the system into phase separation, see Sec. III C.

For smaller  $U$ , as shown for  $U/t = 2$  in Fig. 3, the nature of the charge and spin ordering is less evident. In particular, incommensurate peaks appear in both the  $q_y = \pi$  channel of  $C(\mathbf{q})$  and the  $q_y = 0$  channel of  $S(\mathbf{q})$  as  $V$  is increased. At the largest value shown,  $V/t = 8$ , there are strong oscillations and side peaks in  $C(\mathbf{q})$ . As will be discussed in more detail in Sec. III C, this is due to phase separation between a region of double occupancies on every second site and a region in which individual electrons are mobile. This phase separation occurs for small  $U$  and moderate to large  $V$ , as indicated in the phase diagram of Fig. 1.

## A. Homogeneous phase

First, we concentrate on the states without charge order, i.e., the region of small  $V$  as shown in Fig. 1. The nature of the low-lying excitations can be determined by calculating the energy gaps of the system. In particular, we will consider the charge and spin gaps, defined as

$$\Delta_c = \frac{1}{2} [E_0(L, N+2) + E_0(L, N-2) - 2E_0(L, N)],$$

$$\Delta_s = E_0(L, N, S_z = 1) - E_0(L, N, S_z = 0). \quad (5)$$

Since we calculate the gaps  $\Delta(L)$  on finite systems (of size up to  $L = 80$ ), the gaps must be extrapolated to  $L \rightarrow \infty$ ; we do this by performing a polynomial fit in  $1/L$  through the data points from the larger system sizes ( $L \geq 24$ ). Although we include both  $1/L$  and  $1/L^2$  terms, the coefficient of the quadratic term is quite small in most cases. One such extrapolation is illustrated in Fig. 4, in which we show results for charge and spin gaps at  $U/t_{\parallel} = 8$ ,  $V/t_{\parallel} = 2$  and different values of the hopping ratio  $t_{\perp}/t_{\parallel}$ . We note that the uncertainty of the extrapolated value depends strongly on finite-size effects which become large when the correlation length becomes large; the results for the gaps are most accurate in the strong coupling region,  $U, V \gg t$ . For the spin gap data in Fig. 4, we have verified (by keeping more DMRG states per block and/or using a fit with a  $1/L$  term only) that  $\Delta_s$  vanishes for  $t_{\perp}/t_{\parallel} = 1$ , but is larger than zero for  $t_{\perp}/t_{\parallel} = 0.7$ , within the numerical accuracy available.

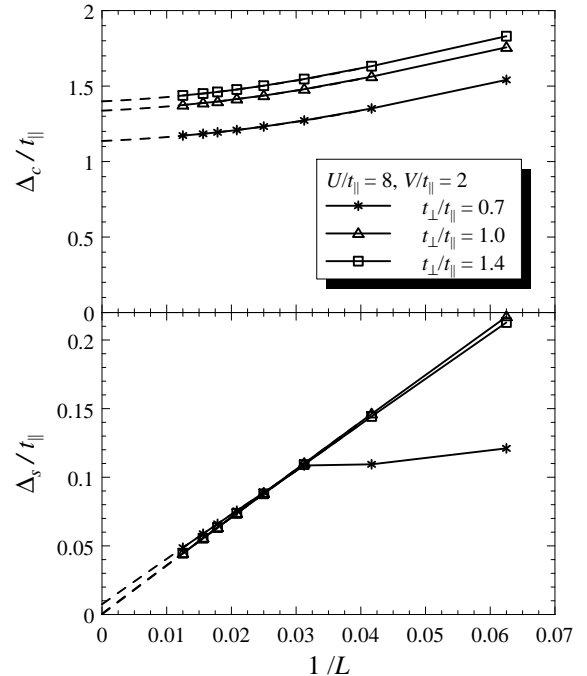


FIG. 4. Finite-size scaling for the charge and spin gaps at  $U/t_{\parallel} = 8$ ,  $V/t_{\parallel} = 2$  and different  $t_{\perp}/t_{\parallel}$ . The solid lines are guides to the eye, the dashed lines are quadratic fits through the data points for  $L = 24$  through 80.

Note that in the weak-coupling limit of the “bare” Hubbard ladder ( $V = 0$ ) in the case of isotropic hopping both spin and charge gaps vanish. As explained above, varying the hopping ratio  $t_{\perp}/t_{\parallel}$  tunes the system through the one-band to two-band transition: For  $t_{\perp} > t_{\parallel}$  Umklapp scattering opens a charge gap (C0S1 phase); with decreasing  $t_{\perp}/t_{\parallel}$  one finds narrow regions of C2S2 and C2S1, followed by a C1S0 phase.<sup>32</sup>

DMRG results for charge and spin gaps in the homogeneous phase are displayed in Fig. 5. For  $V = 0$  we find a C0S1 phase for  $t_{\perp} > t_{\parallel}$  and a C1S0 phase for  $t_{\perp} < 0.9t_{\parallel}$  consistent with the RG predictions of Ref. 32. The data also indicate a narrow region where both  $\Delta_c = 0$  and  $\Delta_s = 0$ , this may correspond to the C2S2 and C2S1 phases. For  $V/t_{\parallel} = 2$  the behavior of the spin gap is similar to the  $V = 0$  case, i.e., it is finite for small  $t_{\perp}$  and vanishes for  $t_{\perp}/t_{\parallel}$  larger than some critical value. However, the charge gap is found to be non-zero for all hopping ratios examined here (see also Figs. 8 and 9 below). Therefore, we conclude that the introduction of  $V$  drives the system to an insulating state even when  $t_{\perp} < t_{\parallel}$ .

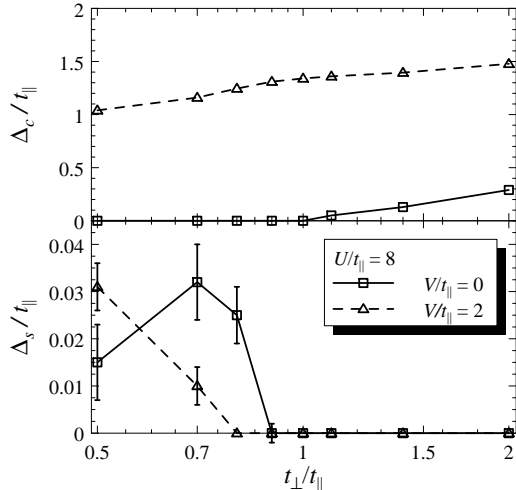


FIG. 5. Charge and spin gaps at  $U/t_{\parallel} = 8$ ,  $V/t_{\parallel} = 0, 2$  as function of the hopping ratio  $t_{\perp}/t_{\parallel}$ . Since the finite-size effects become substantial for small  $t_{\perp}$ , we have indicated the estimated errors from the extrapolation to the thermodynamic limit by error bars. For data points without error bars, the uncertainties are of the order of the symbol size or less.

## B. Charge-ordered phase and ordering transition

As the nearest-neighbor repulsion  $V$  is increased, we expect a transition to a checkerboard charge-ordered state. In order to examine the extent of the charge ordering and the nature of the transition, we calculate the order parameter for  $\mathbf{Q} = (\pi, \pi)$  charge order,

$$\eta = \lim_{L \rightarrow \infty} \frac{C(\mathbf{Q})}{\langle n \rangle^2}. \quad (6)$$

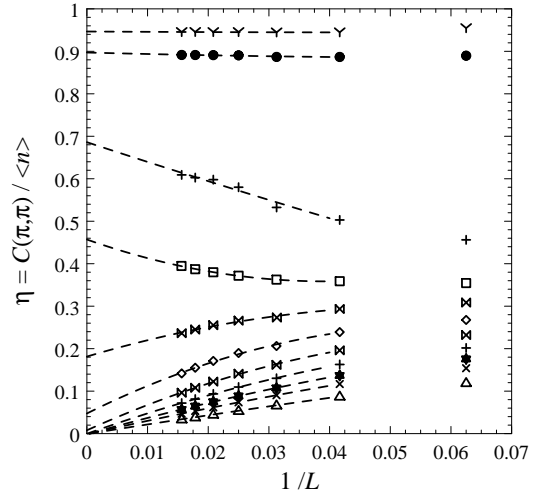


FIG. 6. Finite-size scaling for the staggered charge correlation function at  $U/t = 4$  and isotropic hopping. The curves correspond to  $V/t = 3.0, 3.2, 3.3, 3.4, 3.5, 3.6, 3.7, 3.8, 4.0, 6.0$ , and  $8.0$ , from bottom to top. The dashed lines are quadratic fits through the data points for  $L \geq 24$ .

The extrapolation to the thermodynamic limit,  $L \rightarrow \infty$ , is, as before, performed by fitting a quadratic in  $1/L$  to the values  $\eta(L)$  for  $L \geq 24$ . The deviations from a  $1/L$  behavior are significant only in the immediate vicinity of the charge-order transition, as can be seen in Fig. 6. The extrapolation is the major source of uncertainty in our results for  $\eta$ ; the typical error is approximately  $\Delta\eta = 0.01$ .

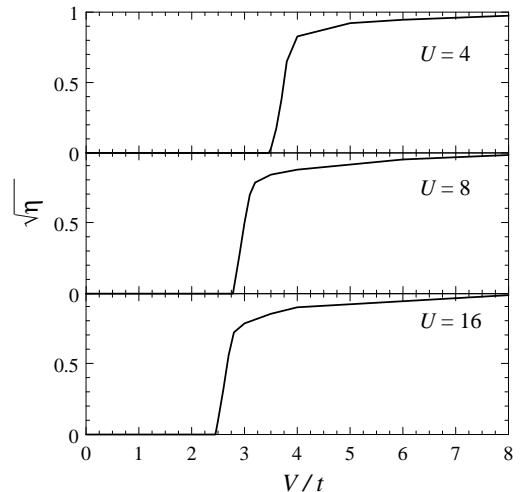


FIG. 7. Order parameter  $\sqrt{\eta}$  versus  $V/t$  for different values of  $U/t$  at quarter filling and isotropic hopping. The data indicate second-order quantum phase transitions between a homogeneous and a charge-ordered state for all  $U$  values shown. The critical parameter values are  $V_c/t = 3.45 \pm 0.1$ ,  $2.8 \pm 0.1$ , and  $2.45 \pm 0.1$  for  $U/t = 4, 8$ , and  $16$ , respectively.<sup>35</sup>

In Fig. 7, we plot the extrapolated values of  $\sqrt{\eta}$  (which correspond to the relative difference of the sublattice occupancies in the broken-symmetry charge-ordered state) for different values of  $U/t$ . The phase transition to a charge-ordered state is always found to be second-order, i.e., the order parameter vanishes continuously at a critical values  $V_c$ . We remind the reader that the transition has been found to change from second-order to first-order at higher band filling as a function of  $U/t$ ;<sup>31</sup> such tricritical behavior has also been observed in the 1D case at half-filling.<sup>20,22</sup>

From the curves of Fig. 7 we obtain  $V_c(U)$ , which are displayed as phase boundaries in Fig. 1. Note that  $V_c$  decreases with increasing  $U$  in the quarter-filled case treated here, similar to the behavior found in 1D.<sup>19</sup> Our results for large  $U$  suggest that  $V_c$  is non-zero in the  $U \rightarrow \infty$  limit; an extrapolation based on data up to  $U/t = 64$  yields  $V_c(U = \infty) \approx 2t$ . It is interesting that at *half filling* weak- and strong-coupling approximations<sup>29,36</sup> as well as numerical studies<sup>22,31</sup> yield  $V_c \approx U/z_0$  for a hypercubic lattice with  $z_0$  being the number of nearest neighbors, i.e., in the half-filled case  $V_c$  *increases* with  $U$ .

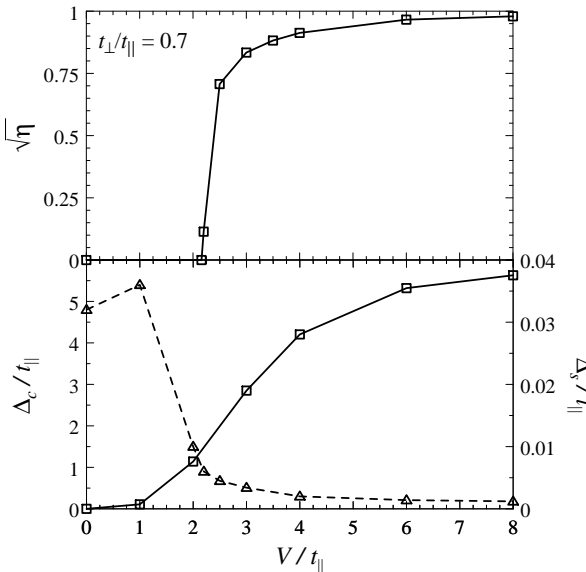


FIG. 8. Order parameter  $\sqrt{\eta}$  (upper panel) and charge (solid) and spin (dashed) gaps (lower panel) as function of  $V/t_{\parallel}$  for  $U/t_{\parallel} = 8$  and  $t_{\perp}/t_{\parallel} = 0.7$ . Although the spin gap decreases when entering the charge-ordered state, it is non-zero for all  $V$ .

The behavior of the low-energy electronic excitations in the vicinity of  $V_c$  provide further information on the character of the charge-order transition. Since the energy gaps show different behavior for different values of the hopping ratio  $t_{\perp}/t_{\parallel}$ , as seen in Fig. 5, we focus on different representative values of the hopping anisotropy. The energy gaps as function of  $V/t_{\parallel}$  together with the order parameter at  $U/t_{\parallel} = 8$  are shown in Figs. 8 and 9 for  $t_{\perp}/t_{\parallel} = 0.7$  and 1.4. The main observation is that no

gap opens or closes at the transition to the charge-ordered state. Small  $t_{\perp}/t_{\parallel}$  leads to fully gapped CO phases on both sides of the transition, whereas at large  $t_{\perp}/t_{\parallel}$  both the homogeneous and the charge-ordered phase have zero spin gap and non-zero charge gap. For the former case (Fig. 8), the spin gap decreases appreciably the charge-ordered state is entered. This indicates a change in the spin dynamics from a “weak-coupling” regime dominated by band effects to a “strong-coupling” regime determined by the physics of a frustrated spin chain. This behavior will be discussed in detail in Sec. IV.

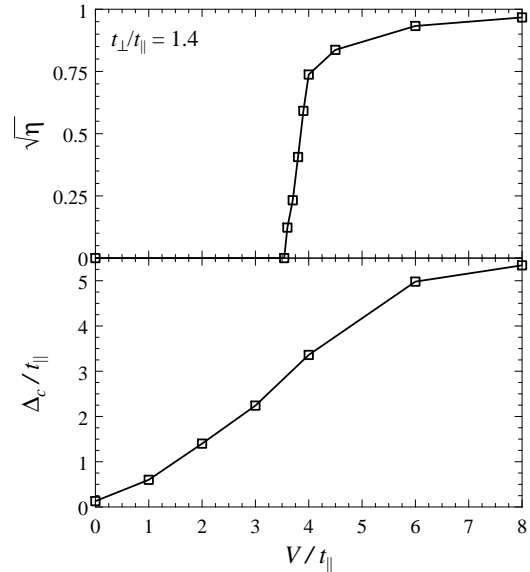


FIG. 9. Same as Fig. 8, but for  $t_{\perp}/t_{\parallel} = 1.4$ . The lower panel now shows the charge gap only; the spin gap is zero within the numerical accuracy for all values of  $V$ .

In any case, it appears that low-lying fermionic excitations do not play a role in the critical dynamics at the charge-order transition. This implies that this zero-temperature transition must be in the universality class of the 1+1-dimensional Ising model. Note, however, that inter-ladder couplings will increase the effective dimensionality of this transition in experimental ladder systems at low enough energies or temperatures.

### C. Phase separation

For small  $U$  and large  $V$ , phase separation is expected: In the  $V \rightarrow \infty$  limit, existing double occupancies are immobile and cannot be broken up, whereas single fermions can move in the “unoccupied” space. For  $U < U_{\text{PS}}(V)$ , the system then separates into a region with double occupancies at every second site (i.e., checkerboard order with two electrons per occupied site) and a region in which the other electrons can gain kinetic energy by hopping. For the one-dimensional system it is possible to solve the  $V = \infty$  problem exactly because it maps onto

non-interacting spinless fermions moving on open chain segments.<sup>19</sup> While the mapping to spinless fermions is similar for the ladder system, the geometry leads to interactions among the fermions which preclude an exact solution. Nevertheless, the qualitative behavior should be similar to the 1D case, i.e., for  $V = \infty$  there should be a critical  $U_{\text{PS}}(\infty)$  ( $U_{\text{PS}}(\infty) = 4t$  in 1D) below which the system phase separates. For small  $V$ , the phase separation should disappear.

We have numerically computed the compressibility of the system which is defined as

$$\kappa = \frac{4L}{N^2} [E_0(L, N+2) + E_0(L, N-2) - 2E_0(L, N)]^{-1}. \quad (7)$$

Our results clearly show the occurrence of phase separation in the large  $V$ , small  $U$  region indicated by (i) a diverging compressibility, (ii) oscillating incommensurate spin and charge correlations with wave vectors strongly dependent on the system size, and (iii) the occurrence of site charge densities greater than unity. Note that at quarter filling no double occupancies occur even in the perfectly charge-ordered state. The appearance of doubly occupied sites in the phase-separated state is clearly consistent with the phase separation mechanism explained above. The criteria (i)–(iii) give consistent results and allow for a reasonable accurate determination of the PS boundary, even though finite size effects in the calculation of the compressibility are large.<sup>19</sup>

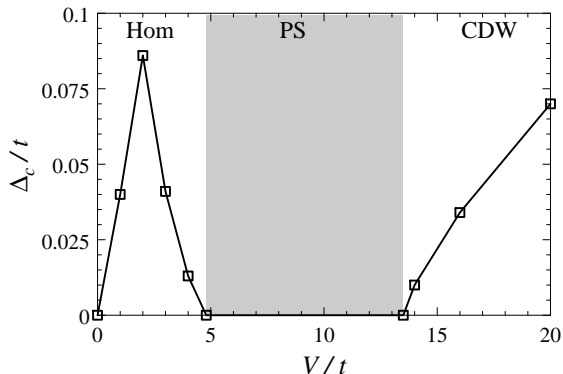


FIG. 10. Charge gap as function of  $V/t$  for  $U/t = 2.2$  and isotropic hopping. There is a homogeneous insulating phase at small  $V$  and a charge-ordered insulating phase at large  $V$ ; an intervening region of phase separation (shaded), characterized by diverging compressibility, is found for  $4.8 < V/t < 13.5$ . In the stable phases, the spin gap is zero to within the numerical accuracy.

In contrast to that found in the 1D chain, the phase separation boundary has non-monotonic behavior, i.e.,  $U_{\text{PS}}(V)$  shows a maximum at around  $V/t \approx 8$ ,  $U/t \approx 2.4$ , as can be seen in Fig. 1. The described “re-entrant” (non-monotonic) behavior of the PS boundary is illustrated in Fig. 10 in which we display the charge gap as a function

of  $V$  for  $U/t = 2.2$ . Here we find a homogeneous phase at small  $V$ , a charge-ordered phase at large  $V$ , and a region of phase separation in between, for  $4.8 < V/t < 13.5$ .

Another difference with the behavior of the single chain extended Hubbard model is that no homogeneous phase appears for large  $V$  and small or intermediate values of  $U$ : increasing  $U$  in the PS region drives the system directly into the charge-ordered state (Fig. 1). In contrast, in the 1D system, a homogeneous phase is present at any  $V$  and the boundaries to the charge-ordered and to the PS phases merge (at  $U/t = 4$ ) only in the  $V \rightarrow \infty$  limit.<sup>19</sup>

For the present ladder system, the behavior at the boundary between the charge-ordered state and the PS region is quite interesting: The charge gap appears to vanish continuously at this boundary (Fig. 10). However, the charge-density wave order parameter  $\sqrt{\eta}$  does not tend to zero when approaching the PS boundary from the charge-order phase. Moreover, the numerical results for small  $U$  (in the PS region) indicate charge density oscillations in the spatial regions without double occupancies; this suggests that strong CDW correlations exist on both sides of the PS boundary, and the transition can be interpreted as “continuous”.

#### IV. STRONG-COUPLING LIMIT

This section focuses on the low-energy spin dynamics at large  $U$  and  $V$  in the checkerboard charge-ordered state. The charge gap in this state can be estimated to be  $\Delta_c = \min(U, 3V)$  when  $t \ll U, V$ , by neglecting the kinetic energy. In this limit, each occupied site in the charge-ordered state carries charge  $e$  and spin  $\frac{1}{2}$ , and the spin states are degenerate for  $V = \infty$ . We would like to discuss the spin ordering arising from effective exchange interactions which occur for small, but finite  $t/V$ . We can do this by treating  $t/V$  as a perturbation, in a manner similar to the derivation of the effective spin exchange in the large- $U$  Hubbard model at *half-filling* which leads to the mapping to an antiferromagnetic Heisenberg model. However, the present problem is slightly more complicated because the degeneracy is lifted in fourth order in the hopping rather than in second order as in the half-filled Hubbard model. The relevant exchange interaction will therefore be of order  $t^4/V^3$  rather than  $t^2/U$ .

The aim is to find an effective Hamiltonian for the residual spin degrees of freedom. It is easy to see that this model will be a frustrated antiferromagnetic Heisenberg  $J_1$ – $J_2$  chain where  $J_1$  and  $J_2$  are a diagonal (1,1) and a horizontal (2,0) coupling between the spins in the checkerboard ordered state. It is well-known<sup>37–40</sup> that this model has a zero-temperature phase transition as a function of  $\alpha = J_2/J_1$ . For  $\alpha < \alpha_c$  the ground state is gapless with power-law correlations. For  $\alpha > \alpha_c$  a spontaneous dimerization occurs which leads to a spin gap and a doubly degenerate ground state. The numerical estimate<sup>38</sup> for  $\alpha_c$  is 0.2411. At  $\alpha = 1/2$  (the Majumdar–

Ghosh point), the ground state has been shown to be an exact product of nearest-neighbor singlets.<sup>41</sup> Therefore, a corresponding spin-gap transition is also possible in the charge-ordered state of the  $t - U - V$  ladder, provided that the effective  $\alpha$  can be tuned through the critical value by changing the system parameters.

We use a recently developed method<sup>42</sup> based on cumulants to derive an effective Hamiltonian for the spin degrees of freedom in the charge-ordered state of the quarter-filled model. We give the derivation in the appendix, and here state only the final result for isotropic nearest-neighbor repulsion,  $V_{\parallel} = V_{\perp} = V$ :

$$\begin{aligned} J_1 &= \frac{2 t_{\perp}^2 t_{\parallel}^2}{V^2} \left\{ \frac{2}{U} + \frac{2}{U + 2V} + \frac{1}{V} \right\} \\ J_2 &= \frac{t_{\parallel}^4}{V^2} \left\{ \frac{1}{U} + \frac{2}{U + 2V} \right\}. \end{aligned} \quad (8)$$

The lowest-order non-zero contributions to  $J_1$  and  $J_2$  are indeed of order  $t^4/V^3$  and terms of order  $t^4/(V^2U)$  also appear. For anisotropic  $V$ , the general expressions become more complicated and are given in the appendix. It turns out that the ratio  $\alpha = J_2/J_1 < 1/4$  for the isotropic case  $t_{\parallel} = t_{\perp}$  and  $V_{\parallel} = V_{\perp}$ ; it approaches  $1/4$  for  $V \gg U \gg t$ , as shown in Fig. 11. The plot shows that the dimerization transition will take place at  $V/U \approx 2$ , however, this transition is hard to observe numerically since the induced gap is very small as we discuss below. To access larger values of  $\alpha$  a hopping anisotropy  $t_{\perp}/t_{\parallel} < 1$  is necessary. The parameter  $\alpha$  can be tuned to any value by varying the hopping ratio.

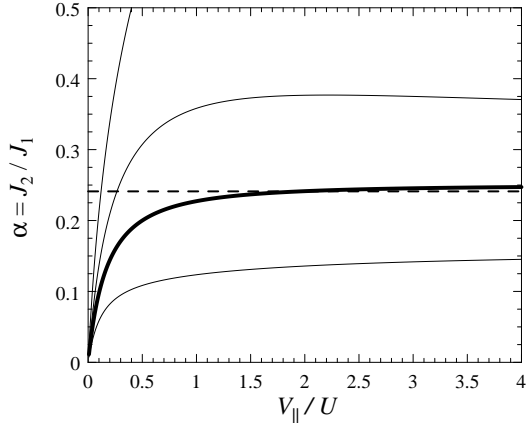


FIG. 11. The ratio of the effective coupling constants  $\alpha = J_2/J_1$  calculated from Eq. (A2) at isotropic hopping. The different curves correspond to  $V_{\perp}/V_{\parallel} = 0, 0.5, 1$  [thick line – see Eq. (8)] and 2 from top to bottom. In order to obtain values for anisotropic hopping,  $\alpha$  must be multiplied by  $(t_{\parallel}/t_{\perp})^2$ . The horizontal dashed line marks the critical value  $\alpha_c = 0.2411$  for the dimerization transition of the frustrated spin chain.

To verify the expressions for  $J_1$  and  $J_2$  given above, we have studied the behavior of the charge-ordered

state in the strong-coupling limit for different hopping anisotropies. In order to interpret results for the spin gap, it is important to note that  $\Delta_s$  in the  $J_1$ – $J_2$  chain vanishes exponentially near the critical point  $\alpha_c$ , leading to nonzero but very small values for  $\alpha < 0.3$ . Therefore, the spin gap calculations in the charge-ordered state require an anisotropy in  $t$  or  $V$  in order to reach  $\alpha$  values significantly larger than 0.3. Furthermore, they are feasible only in a window of intermediate values of  $U/t, V/t$ : overly small values do not lead to a charge-ordered state, whereas overly large values of  $V$  lead to an unobservably small spin gap (of order  $J \sim t^4/V^3$ ).

The nature of the magnetic ground state can also be probed using static spin correlation functions. For the  $J_1$ – $J_2$  chain it is known<sup>39,40</sup> that the static structure factor  $S(\mathbf{q})$  is peaked at  $q = \pi$  for  $\alpha < 1/2$ . For  $\alpha > 1/2$ , the peak position shifts to smaller  $q$  as  $\alpha$  is increased, approaching  $\pi/2$ , the value for two uncoupled chains with a doubled lattice constant, as  $\alpha$  becomes large.

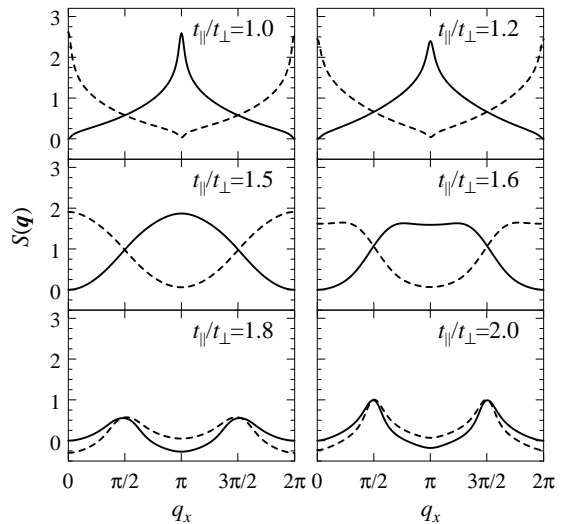


FIG. 12. Spin correlation functions  $S(\mathbf{q})$  in the charge-ordered state of the quarter-filled ladder. As above,  $q_y = 0, \pi$  data are plotted using full and dashed lines, respectively. The parameters are  $L = 64$  and  $U = V = 8t_{\perp}$ , the different values of the hopping ratio  $t_{\parallel}/t_{\perp}$  correspond to effective exchange constants [from (8)] with  $\alpha = J_2/J_1 = 0.227, 0.327, 0.511, 0.582, 0.736$ , and  $0.909$ .

The spin correlations at  $U = V = 8t_{\perp}$  and various hopping ratios obtained from the DMRG calculations are shown in Fig. 12. (Note that we use  $t_{\perp}$  rather than  $t_{\parallel}$  as the energy reference in this section.) A shift of the maximum from  $q_x = \pi$  to  $q_x = \pi/2$  (at  $q_y = 0$ ) with increasing  $t_{\parallel}/t_{\perp}$  is clearly visible. To compare quantitatively with the strong-coupling picture of the frustrated spin chain, we show in Fig. 13 the results for the spin gap  $\Delta_s$  and for the peak position  $q^*$  in the spin structure factor (see Fig. 12) for different parameter sets in the charge-ordered phase. Data for the frustrated spin

chain from Ref. 40 are also shown for comparison. Note that the data are plotted as a function of the ratio  $J_2/J_1$  with the values of these *effective* couplings taken from the strong-coupling expressions (8). The spin gap value follows the strong coupling prediction closely even for intermediate values of  $U/t$  and  $V/t$ . The peak position also shows the expected behavior, i.e., it deviates from  $\pi$  when the effective  $J_2/J_1$  exceeds a certain value. For large  $U$  and  $V$ , the agreement with the results from the frustrated spin chain is nearly perfect, clearly indicating that the spin dynamics in the strong-coupling charge-ordered state is correctly described by the  $J_1$ – $J_2$  spin chain. For smaller values of  $U$  and  $V$ , there are slight deviations in the peak position from the spin chain data: the region of incommensurate spin order becomes narrower with decreasing interaction. This might be expected because there is no incommensurability at half-filling in the non-interacting limit. A similar behavior for  $S(q)$  has been found for the half-filled Hubbard chain with next-nearest-neighbor hopping<sup>43</sup> which can also be mapped onto an effective frustrated spin chain in the large- $U$  limit.

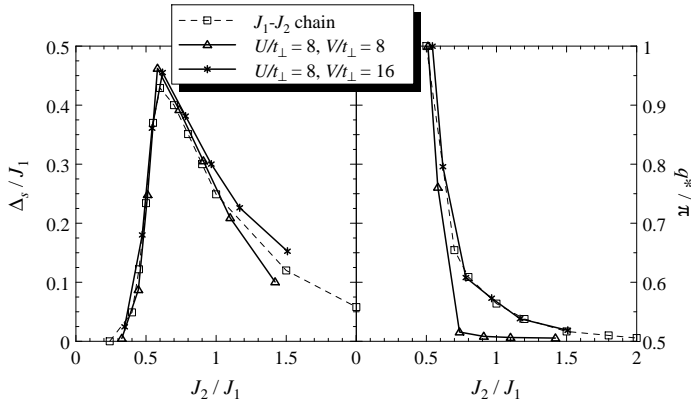


FIG. 13. Spin gap (left) and peak position in the spin structure factor (right) for the charge-ordered state of the quarter-filled  $t$ – $U$ – $V$  ladder. The different curves are obtained by varying the hopping ratio  $t_{\parallel}/t_{\perp}$  at fixed values of  $U/t_{\perp}$  and  $V/t_{\perp}$ . The horizontal axis shows the ratio of the effective exchange constants  $J_1$  and  $J_2$  obtained from the strong-coupling expressions (8). Data marked "J<sub>1</sub>–J<sub>2</sub> chain" are taken from Ref. 40.

Now we turn to a discussion of the special case of isotropic hopping for which the  $V = 0$  weak coupling system is near the one-band to two-band transition. The numerical results obtained by DMRG indicate a zero spin gap and non-zero charge gap for any finite  $V$  (outside the phase-separation region). This is in disagreement with the strong-coupling analysis presented above which predicts that there should be a spin gap in the charge-ordered phase at large  $V/U$  due to spontaneous dimerization. Since  $\alpha = J_2/J_1$  is close to  $\alpha_c$ , however, the gap would be very small and therefore hard to observe using numerical methods. By assuming that the strong-

coupling picture is also valid in the intermediate-coupling regime, we can locate the phase boundary where the spin gap closes in the charge-ordered state. This is shown in Fig. 1. Since it is not possible to deduce the behavior of the spin gap close to the charge-order transition from the current numerical results, we cannot decide whether the charge-order transition line and the spin-gap transition line meet for the case of isotropic hopping. We consider it likely, however, that the region with non-zero spin gap due to dimerization is confined to the charge-ordered phase. Additional numerical approaches (e.g., based on level-crossing methods) could be used to check the spin-gap scenario and to determine the precise location of the boundary of the spin-gap phase.

It is worth pointing out that despite the fact a spin gap is present in both the homogeneous and the charge-ordered phases at small  $t_{\perp}/t_{\parallel}$ , the mechanisms for the spin gap opening appear to be quite different: The strong-coupling transition in the CDW phase involves spontaneous dimerization in a spin model and is described by a sine-Gordon theory, whereas the weak-coupling case at  $V = 0$  is more complicated due to the presence of low-lying charge modes (see Ref. 32 for a discussion on the RG for  $V = 0$ , however, not much is known about the  $V > 0$  case). In this context, we note that additional anisotropy in the nearest-neighbor interaction  $V_{\parallel} \neq V_{\perp}$  modifies the ratio  $J_2/J_1$  as shown in Fig. 11. Such anisotropy can therefore be used to tune the strongly charge-ordered system between the gapless and gapped phases of the frustrated spin- $\frac{1}{2}$  chain.

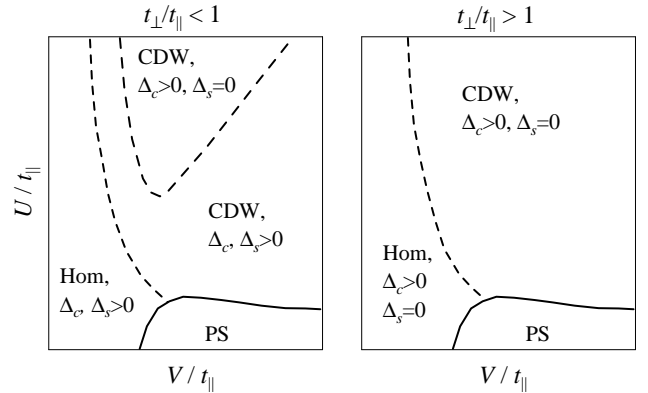


FIG. 14. Proposed schematic phase diagrams for the extended quarter-filled Hubbard model with (large) hopping anisotropy. For  $t_{\perp} < t_{\parallel}$ , the spin gap is non-zero in accordance with the weak coupling predictions, whereas for  $t_{\perp} > t_{\parallel}$  the spin gap is always zero. In the former case, the spin gap can be suppressed deep in the charge-ordered phase if  $V/U$  is smaller than a critical value (which corresponds to  $J_2/J_1 = \alpha < \alpha_c$  for the effective frustrated spin chain).

We conclude this section with a brief discussion of the phase diagrams for the anisotropic hopping cases. While we have not mapped out the full phase diagram for  $t_{\perp}/t_{\parallel} \neq 1$ , some features are clear from the above con-

siderations and from the numerical results obtained for  $t_{\perp}/t_{\parallel} = 0.7$  and  $1.4$ . The homogeneous phase appears to be insulating for all  $U, V > 0$ . (Note that  $V = 0$  leads to a metallic, spin-gapped phase at small  $t_{\perp}/t_{\parallel}$ ). Phase separation will occur for small  $U$  and large  $V$  for any non-zero hopping  $t_{\parallel}$ . The main effect of varying  $t_{\perp}/t_{\parallel}$  is therefore on the spin gap: The homogeneous phase has a transition as function of the hopping ratio where the spin gap opens. This critical hopping ratio may depend on the interaction strength, but is probably near unity for reasonable values of the interactions. (We have not systematically studied this so far; see Fig. 5 for some values). The charge-ordered phase follows the strong-coupling predictions described in this section. Here, no spin gap occurs for large  $t_{\perp}/t_{\parallel}$  whereas small  $t_{\perp}/t_{\parallel}$  leads to a spin gap for sufficiently large values of  $V/U$ . From this considerations, we propose the schematic phase diagrams for the  $t_{\perp} < t_{\parallel}$  and  $t_{\perp} > t_{\parallel}$  cases which are displayed in Fig. 14.

## V. CONCLUSIONS

In summary, we have studied the phase diagram of the extended Hubbard model on a quarter-filled two-leg ladder. Our main findings are that at small interactions, the system is insulating with either zero or non-zero spin gap depending on the hopping anisotropy. At large  $V$  and not too small  $U$ , the ground state shows zig-zag charge order. In this phase each occupied site carries spin  $\frac{1}{2}$  and the residual kinetic energy leads to effective antiferromagnetic exchange interactions between the spins which can be represented as a frustrated  $J_1$ - $J_2$  spin chain. Depending on the model parameters, this effective spin chain can be either in the gapless regime with algebraic spin correlations or in the spontaneously dimerized regime with gapped spin excitations. Finally, at small values of  $U$  and moderate to large values of  $V$ , the system phase separates into a phase of immobile double occupancies on every second site and a phase of mobile single electrons.

We have rigorously established the mapping of the spin degrees of freedom in the charge ordered state to the frustrated spin- $\frac{1}{2}$  chain in the strong coupling limit,  $U, V \gg t$ . In addition, we have shown that the physics of the frustrated Heisenberg chain is also observed in the intermediate coupling regime. For anisotropic hopping,  $t_{\perp} < t_{\parallel}$ , the charge-ordered system spontaneously dimerizes and the spin gap in the charge-ordered state could be numerically observed. Its magnitude is in good agreement with the results for a corresponding frustrated spin chain down to  $U/t = 4$ . The dimerization of the effective spin chain can be interpreted as bond-order wave<sup>44</sup> in the original Hubbard model, so the system has an insulating ground state with coexisting bond-order and charge-density wave.

We have identified a purely electronic mechanism for the opening of a spin gap in a quarter-filled CDW sys-

tem on a ladder based on the physics of a frustrated spin chain. However, we note here that the spin-gap physics discussed in Sec. IV probably cannot be realized in  $\text{NaV}_2\text{O}_5$  since this material has  $t_{\perp} \approx 2t_{\parallel}$  (see Refs. 4,45) leading to  $J_1 \gg J_2$  for the effective spin chain. It is likely that the spin gap opening in  $\text{NaV}_2\text{O}_5$  is driven by the interplay of charge ordering and phonons, as suggested in Ref. 45. Other effects which are probably important for the spin dynamics in  $\text{NaV}_2\text{O}_5$  are hopping processes between the ladders which may lead to quite large exchange terms across the ladders.<sup>11</sup>

We have found no evidence for “exotic” phases in the examined ladder system like the ones present in the single-chain model.<sup>19,25</sup> Furthermore, there appears to be no metallic phase in the quarter-filled model for finite repulsive  $U$  and  $V$ ; similarly, a phase with dominant superconducting fluctuations can also be excluded.

Any effects of interladder couplings have been neglected in the present treatment, as well as the interplay of electron and lattice effects which is known to lead to further interesting ordering effects;<sup>46</sup> these should be investigated in the future. Also, a more detailed study of the spin dynamics in a partially charge-ordered state ( $V < \infty$ ) could be performed.

## ACKNOWLEDGMENTS

The authors thank D. Baeriswyl, R. Bulla, P. G. J. van Dongen, R. E. Hetzel, and A. P. Kampf for useful conversations. M.V. acknowledges support by the DFG (VO 794/1-1) and by US NSF Grant No DMR 96-23181, R.M.N. has been supported by the Swiss National Foundation under Grant No 20-53800.98. The calculations were performed on the Origin 2000 at the Technical University Dresden.

## APPENDIX A: EFFECTIVE HAMILTONIAN FOR THE CHARGE-ORDERED STATE

This appendix provides the derivation of the effective exchange Hamiltonian for the quarter-filled ladder in the strongly charge-ordered regime,  $(V, U) \gg t$ . The charge degrees of freedom are projected out, i.e., the effective Hamiltonian  $\mathcal{H}_{\text{eff}}$  acts in a Hilbert space where every second site is singly occupied. This is analogous to the derivation of the Heisenberg model as large- $U$  limit of the half-filled one-band Hubbard model. The present problem maps onto a frustrated  $J_1$ - $J_2$  spin chain. The effective exchange arises from fourth-order hopping processes which makes the problem more complicated than the half-filled Hubbard model for which the lowest non-trivial contributions arise at second order in  $t$ .

We apply a recently developed cumulant method<sup>42</sup> to derive  $\mathcal{H}_{\text{eff}}$ . It is useful to split  $\mathcal{H} = \mathcal{H}_0 + \mathcal{H}_1$  where  $\mathcal{H}_0$  contains the dominating interaction terms and  $\mathcal{H}_1$

the perturbation caused by hopping. We start with broken translational symmetry from the outset and define a projection operator  $\mathcal{P}$  which projects onto the low-energy space where the charges show perfect checkerboard charge order, i.e.,  $\langle n_i \rangle = [1 + \exp(i\mathbf{Q}\mathbf{R}_i)]/2$  with  $\mathbf{Q} = (\pi, \pi)$ . This order defines two sublattices which we will denote as  $A$  and  $B$  for occupied and unoccupied, respectively. Transitions between states within the  $\mathcal{P}$  space are only possible with four or more hopping processes; the fourth order processes only involve intermediate states outside the  $\mathcal{P}$  space. The fourth-order Hamiltonian can be obtained by fourth-order perturbation theory and is given by<sup>42</sup>

$$\mathcal{H}_{\text{eff}} = -\mathcal{P}\mathcal{H}_1\mathcal{Q}\frac{1}{\mathcal{H}_0}\mathcal{Q}\mathcal{H}_1\mathcal{Q}\frac{1}{\mathcal{H}_0}\mathcal{Q}\mathcal{H}_1\mathcal{Q}\frac{1}{\mathcal{H}_0}\mathcal{Q}\mathcal{H}_1\mathcal{P}, \quad (\text{A1})$$

where  $\mathcal{Q} \equiv 1 - \mathcal{P}$ .

This expression can be easily used to identify the processes contributing to the effective exchange. We first discuss the fourth-order processes leading to  $J_2$ , i.e., the processes coupling two spins located on the same leg of the ladder. They involve exactly one site in between the two originally occupied sites. Therefore, any fourth order hopping process must involve a temporary double occupancy. A suitable classification of the possible processes is shown in Fig. 15.

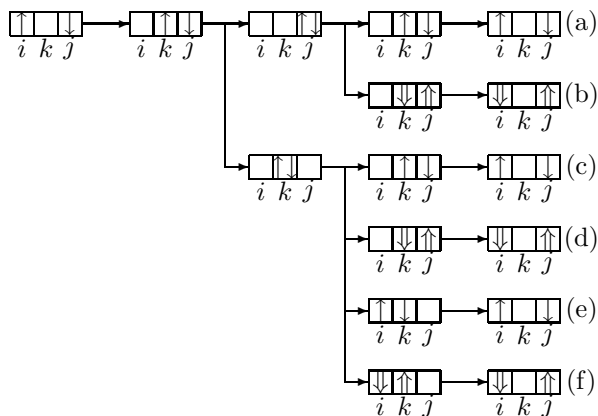


FIG. 15. Processes contributing to  $J_2$ . Here,  $i, j \in A$  are the originally occupied lattice sites whereas  $k \in B$  is the intermediate site.  $\uparrow$  and  $\downarrow$  denote spins being reversed with respect to the initial configuration.

Any process involves three transition states giving rise to the energy denominator of the final expression for  $J_2$ . It is easy to see that (a) and (b) have transition states with energies  $V_{\parallel} + V_{\perp}$ ,  $U$ , and  $V_{\parallel} + V_{\perp}$  (the  $V_{\perp}$  arises from the nearby occupied site on the second leg) whereas (c)-(f) have transition state energies  $V_{\parallel} + V_{\perp}$ ,  $U + 2V_{\perp}$ , and  $V_{\parallel} + V_{\perp}$ . The sum of all processes has the form  $J_2(n_{i,\sigma}n_{j,-\sigma} + c_{i,\sigma}^\dagger c_{i,-\sigma} c_{j,\sigma} c_{j,-\sigma}^\dagger)$ . Examination of the signs shows that the resulting exchange is antiferromagnetic,  $J_2 > 0$ . For the  $J_1$  processes there are two intermediate empty sites in between the two occupied sites

Therefore, processes involving one or both of these two sites are possible. Particularly interesting are the circular hopping processes contributing to the diagonal exchange  $J_1$  in which both intermediate sites are involved and *no* temporary double occupancy occurs. These processes include four sites and the two electrons under consideration are never on the same site. Nevertheless, these processes lead to an effective spin–spin interaction  $\mathbf{S}_1 \cdot \mathbf{S}_2$  (and not only a constant energy shift): For parallel spins the process reproduces the original state, whereas antiparallel spins are *always* exchanged. This leads to the exchange form  $S_1^- S_2^+ + S_1^+ S_2^- + 2(S_1^z S_2^z + 1/2)$ .

For isotropic hopping and interaction, these considerations can be summarized to  $J_1 = 2J_2 + J_{\text{circ}}$ , where  $J_{\text{circ}}$  arises from the circular hopping processes; in the general anisotropic case the  $J_1$  processes will have energy denominators different from the ones quoted above. Collecting all terms leads to the following (general) result for the exchange couplings:

$$\begin{aligned} J_1 &= 4t_{\perp}^2 t_{\parallel}^2 \left\{ \left( \frac{1}{U} + \frac{1}{U + 2V_{\parallel}} \right) \left( \frac{1}{(2V_{\parallel})^2} + \frac{1}{V_{\parallel}(V_{\perp} + V_{\parallel})} + \frac{1}{(V_{\parallel} + V_{\perp})^2} \right) + \frac{1}{V_{\parallel}^2(V_{\perp} + V_{\parallel})} \right\} \\ J_2 &= \frac{4t_{\parallel}^4}{(V_{\parallel} + V_{\perp})^2} \left\{ \frac{1}{U} + \frac{2}{U + 2V_{\perp}} \right\}. \end{aligned} \quad (\text{A2})$$

For isotropic repulsion,  $V_{\parallel} = V_{\perp}$ , these expressions reduce to Eq. (8) quoted in the body of the paper.

\* New permanent address: Theoretische Physik III, Elektronische Korrelationen und Magnetismus, Universität Augsburg, D-86135 Augsburg, Germany.

<sup>1</sup> T. Ohama, H. Yasuoka, M. Isobe, and Y. Ueda, Phys. Rev. B **59**, 3299 (1999).

<sup>2</sup> M. Isobe and Y. Ueda, J. Phys. Soc. Jpn. **65**, 1178 (1996).

<sup>3</sup> Y. Fujii *et al.*, J. Phys. Soc. Jpn. **66**, 326 (1997).

<sup>4</sup> H. Smolinski, C. Gros, W. Weber, U. Peuchert, G. Roth, M. Weiden, and C. Geibel, Phys. Rev. Lett. **80**, 5164 (1998).

<sup>5</sup> H. Seo and H. Fukuyama, J. Phys. Soc. Jpn. **67**, 2602 (1998).

<sup>6</sup> E. Dagotto and T. M. Rice, Science **271**, 618 (1996).

<sup>7</sup> T. Ohama, A. Goto, T. Shimizu, E. Ninomiya, H. Sawa, M. Isobe, and Y. Ueda, cond-mat/0003141.

<sup>8</sup> H. Nakao *et al.*, cond-mat/0003129.

<sup>9</sup> B. Grenier, O. Cepas, L. P. Regnault, J. E. Lorenzo, T. Ziman, J. P. Boucher, A. Hiess, T. Chatterji, J. Jegoudez, and A. Revcolevschi, cond-mat/0007025.

<sup>10</sup> C. Gros and R. Valenti, Phys. Rev. Lett. **82**, 976 (1999).

<sup>11</sup> P. Thalmeier and A. N. Yaresko, Eur. Phys. J. B **14**, 495 (2000).

<sup>12</sup> S. van Smaalen and J. Lüdecke, *Europhys. Lett.* **49**, 250 (2000).

<sup>13</sup> M. Köppen *et al.*, *Phys. Rev. B* **57**, 8466 (1998).

<sup>14</sup> P. Thalmeier and P. Fulde, *Europhys. Lett.* **44**, 242 (1998).

<sup>15</sup> J. L. de Boer, A. Meetsma, J. Baas, and T. T. M. Palstra, *Phys. Rev. Lett.* **84**, 3962 (2000).

<sup>16</sup> C. Gros, R. Valenti, J. V. Alvarez, K. Hamacher, and W. Wenzel, *cond-mat/0004404*.

<sup>17</sup> J. Hubbard, *Phys. Rev. B* **17**, 494 (1978).

<sup>18</sup> F. Mila and X. Zotos, *Europhys. Lett.* **24**, 133 (1993).

<sup>19</sup> K. Penc and F. Mila, *Phys. Rev. B* **49**, 9670 (1994).

<sup>20</sup> J. W. Cannon, R. T. Scalettar, and E. Fradkin, *Phys. Rev. B* **44**, 5995 (1991).

<sup>21</sup> J. E. Hirsch, *Phys. Rev. Lett.* **53**, 2327 (1984); *Phys. Rev. B* **31**, 6022 (1985).

<sup>22</sup> G. P. Zhang, *Phys. Rev. B* **56**, 9189 (1997).

<sup>23</sup> M. Nakamura, *J. Phys. Soc. Jpn.* **68**, 3123 (1999), *Phys. Rev. B* **61**, 16377 (2000), *cond-mat/0003419*.

<sup>24</sup> H. Q. Lin, E. R. Gagliano, D. K. Campbell, E. H. Fradkin, and J. E. Gubernatis in *The Hubbard Model, its Physics and Mathematical Physics*, edited by D. Baeriswyl *et al.*, NATO ASI Series (Plenum, New York, 1995).

<sup>25</sup> R. T. Clay, A. W. Sandvik, and D. K. Campbell, *Phys. Rev. B* **59**, 4665 (1999).

<sup>26</sup> Y. Zhang and J. Callaway, *Phys. Rev. B* **39**, 9397 (1989).

<sup>27</sup> B. Chattopadhyay and D. M. Gaitonde, *Phys. Rev. B* **55**, 15364 (1997).

<sup>28</sup> R. Pietig, R. Bulla, and S. Blawid, *Phys. Rev. Lett.* **82**, 4046 (1999).

<sup>29</sup> P. G. J. van Dongen, *Phys. Rev. B* **49**, 7904 (1994); *Phys. Rev. B* **50**, 14016 (1994).

<sup>30</sup> P. G. J. van Dongen, *Phys. Rev. B* **54**, 1584 (1996).

<sup>31</sup> M. Vojta, R. E. Hetzel, and R. M. Noack, *Phys. Rev. B* **60**, R8417 (1999).

<sup>32</sup> L. Balents and M. P. A. Fisher, *Phys. Rev. B* **53**, 12133 (1996).

<sup>33</sup> R. M. Noack, S. R. White, and D. J. Scalapino, *Physica C* **270**, 281 (1996).

<sup>34</sup> S. R. White, *Phys. Rev. Lett.* **69**, 2863 (1992), *Phys. Rev. B* **48**, 10345 (1993).

<sup>35</sup> The present  $V_c$  values are more accurate and slightly larger than the ones reported in Ref. 31; this is due to more data points and the additional quadratic term for the  $1/L$  finite-size extrapolation.

<sup>36</sup> D. Cabib and E. Callen, *Phys. Rev. B* **12**, 5249 (1971); R. A. Bari, *Phys. Rev. B* **3**, 2662 (1971).

<sup>37</sup> F. D. M. Haldane, *Phys. Rev. B* **25**, 4925 (1982), I. Affleck, D. Gepner, H. J. Schulz, and T. Ziman, *J. Phys. A* **22**, 511 (1989).

<sup>38</sup> S. Eggert and I. Affleck, *Phys. Rev. B* **46**, 10866 (1992), S. Eggert, *Phys. Rev. B* **54**, 9612 (1996).

<sup>39</sup> R. Chitra, S. Pati, H. R. Krishnamurthy, D. Sen, and S. Ramasesha, *Phys. Rev. B* **52**, 6581 (1995).

<sup>40</sup> S. R. White and I. Affleck, *Phys. Rev. B* **54**, 9862 (1996).

<sup>41</sup> C. K. Majumdar and D. K. Ghosh, *J. Math. Phys.* **10**, 1388 (1969).

<sup>42</sup> A. Hübsch, M. Vojta, and K. W. Becker, *J. Phys. Cond. Matter* **11**, 8523 (1999).

<sup>43</sup> S. Daul and R. M. Noack, *Phys. Rev. B* **61**, 1646 (2000).

<sup>44</sup> S. Mazumdar, S. Ramasesha, R. T. Clay, D. K. Campbell, *Phys. Rev. Lett.* **82**, 1522 (1999), S. Mazumdar, R. T. Clay, and D. K. Campbell, *cond-mat/9910164*, *cond-mat/0003200*.

<sup>45</sup> M. V. Mostovoy and D. I. Khomskii, *Solid State Commun.* **113**, 159 (2000).

<sup>46</sup> J. Riera and D. Poilblanc, *Phys. Rev. B* **59**, 2667 (1999).